Inorg. Chem. **2006**, *45*, 8958–8964

Electronic Stabilization Effects: Three New K–In–T (T = Mg, Au, Zn) Network Compounds

Bin Li and John D. Corbett*

Ames Laboratory, Department of Energy,[1] and Department of Chemistry, Iowa State University, Ames, Iowa 50011

Received June 16, 2006

The ternary compounds $K_{34}In_{91.05(9)}Mg_{13.95(9)}$ (**I**), $K_{34}In_{96.19(6)}Au_{8.81(6)}$ (**II**), and $K_{34}In_{89.95(1)}Zn_{13.05(7)}$ (**III**) have been synthesized by high-temperature means and structurally characterized by single-crystal X-ray diffraction methods. All are analogues of earlier products in which Li is substituted for some In in a hypothetical $K_{34}In_{105}$ lattice. They consist of complex three-dimensional anionic networks built of In_{12} icosahedra and M_{28} triply fused icosahedra (M = In or In/T and T = Mg, Au, or Zn). The K atoms bridge between cluster faces or edges and form K_{136} clathrate-II type networks. Two neighboring M_{28} units are interconnected by an M atom to form a sandwich complex $(M_{28})M(M_{28})$ in **I** and **II** or by a Zn–Zn dimer in $(M_{28})ZnZn(M_{28})$ in **III**. Mixed In/T sites only occur in the M_{28} portions. Phase stabilization through electronic tuning is present in all three via substitution of the electron-poorer T elements for In. Extended Hückel analyses indicate that all metal–metal bonding within the M_{28} cluster appears to be optimized in **I** and **III** even though both are metallic. The size of the substituted element is also important in the structural features, as is especially shown by the Zn compound.

Introduction

Previous studies of alkali-metal−triel (group 13 element) systems have shown that the triel usually forms clusters that are interbonded or linked into three-dimensional network structures in which the cations reside in cavities among the clusters.[2] These intermetallic compounds usually exhibit some degree of "electronic deficiency" through the formation of multicenter bonds in clusters. However, these phases also exhibit, or closely approach, closed-shell electronic configurations as a driving force for the creation of these extensive networks. These may be generated in different ways, such as by the formation of vacancies at specific cluster sites or through substitution of even modest amounts of electron-poorer elements in the clusters. For example, the tubular clusters, $(In/Cd)_{18}$ and $(Ga/Ag)_{18}$, have been found in $Na_8K_{23}Cd_{12}In_{48}$[3] and $Na_{30}(Ga_{56}Ag_4)$,[4] respectively, and different kinds of M_{60} (M = Al/Zn or Tl/Cd) buckyballs occur in $Mg_{2-y}(Zn_xAl_{1-x})_{3+y}$[5] and $Na_{13}(Cd_{\sim 0.70}Tl_{\sim 0.30})_{27}$[6] with Bergman-type structures.

The triply fused icosahedral M_{28} is another good illustration of the formation of a large and condensed cluster through either substitution of electron-poorer elements or vacancy formation. For example, the condensed clusters $(Ga/M)_{28}$ were found in $Na_{102}(MGa)_{315}$ (M = Cu, Zn)[7] and related unprecedented $(In/Li)_{28}$ polyhedra were discovered in $K_{14}Na_{20}In_{91.82}Li_{13.18}$ and $K_{34}In_{92.30}Li_{12.70}$ in our recent explorations.[8] Triply fused icosahedra with vacancies as Ga_{28-x} and In_{28-x} were also found in $K_4Na_{13}Ga_{49.57}$[9] and $K_{14}Na_{20}In_{96.30}$,[8] respectively. These triply fused icosahedral clusters are reminiscent of the polyborons in β-B and can be considered as extensions of anionic boron hydride chemistry[10] into H-free intermetallic solids. For convenience, we propose that

* To whom correspondence should be addressed. E-mail: jcorbett@iastate.edu.

(1) This research was supported by the Office of the Basic Energy Sciences, Materials Sciences Division, U.S. Department of Energy (DOE). The Ames Laboratory is operated for DOE by Iowa State University under Contract W-7405-Eng-82.

(2) Corbett, J. D. In *Chemistry, Structure and Bonding of Zintl Phases and Ions*; Kauzlarich, S., Ed.; VCH Publishers: New York, 1996; Chapter 3. Corbett, J. D. *Angew. Chem., Int. Ed.* **2000**, *39*, 670. Belin, C. H. E.; Charbonnel, M. *Prog. Solid State Chem.* **1993**, *22*, 59.

(3) Flot, D. M.; Tillard-Charbonnel, M.; Belin, C. H. E. *J. Am. Chem. Soc.* **1996**, *118*, 5229.

(4) Henning, R. W.; Corbett, J. D. *Z. Anorg. Allg. Chem.* **2002**, *628*, 2715.

(5) Lee, C.-S.; Miller, G. J. *J. Am. Chem Soc.* **2000**, *122*, 4937. Lee, C.-S.; Miller, G. *Inorg. Chem.* **2001**, *40*, 338.

(6) Li, B.; Corbett, J. D. *Inorg. Chem.* **2004**, *43*, 3582.

(7) Charbonnel, M.; Chouaibi, N.; Belin, C. *J. Solid State Chem.* **1992**, *100*, 220. Charbonnel, M.; Chouaibi, N.; Belin, C. *C. R. Acad. Sci. Paris* **1992**, *315*, 661.

(8) Li, B.; Corbett, J. D. *J. Am. Chem. Soc.* **2005**, *127*, 926.

(9) Belin, C. H. E.; Charbonnel, M. *J. Solid State Chem.* **1986**, *64*, 57.

(10) Jemmis, E. D.; Balkarishnarajan, M. M.; Pancharatna, P. D. *Chem. Rev.* **2002**, *102*, 93.

10.1021/ic061089y CCC: $33.50
Published on Web 09/30/2006

all of the phases containing triply fused icosahedra be called *tri-icosahedral phases*.

Our further studies of alkali−metal−In systems show that electronic tuning through the substitution of the electron-poorer elements for In is a very useful and general way to stabilize tri-icosahedral phases. Here we extend our discoveries with Li[8] to Mg, Au, or Zn in the analogous derivatives $K_{34}In_{91.05(9)}Mg_{13.95(9)}$ (**I**), $K_{34}In_{96.19(6)}Au_{8.81(6)}$ (**II**), and $K_{34}In_{89.95(1)}Zn_{13.05(7)}$ (**III**). Bonding optimization in the structures further demonstrates the intimate relationship between the structure and valence electron counts.

Experimental Section

Syntheses. All materials were handled in N_2-filled gloveboxes that had moisture levels below 1 ppm (by volume). The new compounds were synthesized via high-temperature reactions of the pure elements (99.95% K chunks, 99.99% In, 99.98% Zn, 99.98% Mg as tear drops, and 99.99% Au blocks, all from Alfa-Aesar). The weighed elements were enclosed in Ta tubes that were in turn welded shut and sealed within evacuated fused-silica jackets by methods and techniques described previously.[11]

The single-crystal analyses were obtained from the products of $K_{34}In_{79}M_{26}$ (M = Mg or Zn) and $K_{34}In_{92}Au_{13}$ reactions, all of which were expected to give phases with 969 valence electrons, close to that in the presumed isostructural compound $K_{34}In_{92.30}Li_{12.70}$.[8] However, the compositions obtained from the single-crystal refinements were all different. Once the stoichiometries had been established from crystallography, a high-purity phase of each (>95%) was obtained (according to comparisons of their Guinier powder patterns with those calculated from the refined structures). All compounds are very sensitive to traces of moisture and air at room temperature, and all thereby yield minor amounts of KIn_4 that show diffuse powder patterns. All compounds are silvery and brittle and can be made by heating the appropriate mixture at 700 °C for 4 h, then cooling at 10 °C/h to 250 °C, and annealing them for 160 h to grow crystals. Attempts to synthesize the isostructural[8] quaternary Na−K−In−M (M = Mg, Zn, Au) and ternary K−In−M (M = Cu, Ag) compounds failed.

X-ray powder diffraction data were collected with the aid of a Huber 670 Guinier powder camera equipped with an area detector and Cu Kα radiation (λ = 1.540 598 Å). Powdered samples were homogeneously dispersed between two layers of Mylar with the aid of a little vacuum grease. The step size was set at 0.005°, and the exposure time was 0.5 h. Data acquisition was controlled via the in situ program. Peak search, indexing, and least-squares refinements for cell parameters were done with the *Rietica* program.[12] Even though all three structures exhibit some mixing in In positions by Mg, Zn, or Au, there was no evidence of any nonstoichiometry according to a shift of any cell parameters in samples loaded with different proportions, as judged from either their single-crystal or powder pattern refinements. Actually, all other tri-icosahedral phases have also been reported to be line phases with either mixed atoms or partial occupancies.[7−9]

Structure Determination. Single-crystal diffraction techniques were used for detailed structural analyses. Diffraction data for compounds **II** and **III** were collected at 293 K with the aid of a Bruker SMART APEX CCD diffractometer and Mo Kα radiation and were harvested from three sets of 606 frames with 0.3° scans in ω and exposure times of 10 s/frame. The 2θ range extended from 3° to 57°. The unit cell parameters for each were determined from about 900 indexed reflections. The reflection intensities were integrated with the *SAINT* subprogram in the *SMART* software package.[13] The data were corrected for Lorentz and polarization effects and for absorption empirically by the program *SADABS*.[14] Diffraction data for compound **I** were collected at 293 K with the aid of a Stoe IPDS II single-crystal X-ray diffractometer with Mo Kα radiation. Data collection and integration were carried out using the supplied Stoe software. The data were corrected for Lorentz and polarization effects and for absorption numerically with the program *X-shape* in the software included.[15] All three structure solutions were obtained by direct methods and refined by full-matrix least-squares refinement of F_o^2 with the Bruker *SHELXTL* 6.1 software package.[16]

The observed extinction conditions and intensity statistics for all three diffraction data sets were consistent with a $R\bar{3}m$ space group, and this gave satisfactory refinement results. For **I**, direct methods provided 14 peaks with distances among them that were appropriate for In atoms, and they were so assigned. A few least-squares cycles followed by a difference Fourier map revealed seven less strongly diffracting for which distances about six were appropriate for K atoms and another one for Mg, and they were so assigned. However, it became clear after a few more cycles that In alone had too many electrons for the In4, In12, and In15 sites, and Mg alone, too few for the M13 position. At this point, R1 and the highest difference peak were 0.081 and 8.22 e/Å^3, respectively. Allowing constrained mixtures of Mg and In to refine at these four positions, with varying isotropic displacement parameters, gave significant improvements in R1 (0.052) and the highest difference peak (7.06 e/Å^3, 1.23 C from M15). Refinement, finally with anisotropic displacement parameters for all atoms, converged R1 = 0.0355 and wR2 = 0.0603 and gave the same residual peak of 3.51 e/Å^3. It is more reasonable to refine these positions as mixed Mg and In than K and In considering the large electronegativity differences between K and In. Other recent research has also shown that Mg preferentially forms anionic clusters with In in the structures of $Rb_{14}Mg_{4.5}In_{25.5}$,[17] $K_3Mg_{20}In_{14}$,[18] and $AeMg_5In_3$ (Ae = Ba, Sr).[19] Similarly, the structure of **II** was refined with Au15 fully occupied and two crystallographic positions, M11 and M12, co-occupied by Au and In. Its final refinement with anisotropic displacement parameters for all atoms converged R1 = 0.0294 with the largest residual peak, 3.03 e/Å^3, at 1.23 C from In14.

For **III**, direct methods provided 12 peaks with distances to each other that were appropriate for In atoms and one for a Zn atom, and they were so assigned (In1−In11, Zn12, and In14). A few least-squares cycles followed by a difference Fourier map revealed seven less strongly diffracting atoms with distances where about six of them were appropriate for K atoms and another one for Zn, and they were so assigned. At this point, R1 and the highest difference peak were 0.0773 and 14.6 e/Å^3, respectively. After a few more cycles, it became clear that In and Zn were too electron-rich for the In11 and Zn13 positions, respectively. Allowing Zn to admix at the In11 position and varying the occupancy of Zn13 and all

(11) Dong, Z.-C.; Corbett, J. D. *J. Am. Chem. Soc*. **1993**, *115*, 11299.
(12) Howard, C. J.; Hunter, B. A. *LHPM-Rietica Rietveld*, version 1.71; Lucas Heights Research Laboratories: New South Wales, Australia, 1997.
(13) *SMART*; Bruker AXS, Inc.; Madison, WI, 1996.
(14) Blessing, R. H. *Acta Crystallogr*. **1995**, *A51*, 33.
(15) *IPDS II*; Stoe and Cie Gmbh: Darmstadt, Germany, *2002*. *X-shape*: *Crystal Optimistion for Numerical Absorption Correction*, revision 2.03; Stoe and Cie Gmbh: Darmstadt, Germany, 2003.
(16) *SHELXTL*; Bruker AXS, Inc.; Madison, WI, 2000.
(17) Li, B.; Corbett, J. D. *Inorg. Chem.* **2006**, *45*, 156.
(18) Li, B.; Corbett, J. D. *Inorg. Chem.* **2006**, *45*, 3861.
(19) Li, B.; Corbett, J. D., manuscript in preparation.

Table 1. Single-Crystal and Structure Refinement Data for $K_{34}In_{91.05(9)}Mg_{13.95(9)}$ (**I**), $K_{34}In_{96.19(6)}Au_{8.81(6)}$ (**II**), and $K_{34}In_{89.95(1)}Zn_{13.05(7)}$ (**III**)

compound	**I**	**II**	**III**
fw	12125.00	14109.21	12510.37
space group, Z		$R\bar{3}m$ (No. 166), 3	
a (Å)[a]	18.750(3)	18.4741(4)	18.4391(8)
c (Å)	40.547(8)	39.960(2)	40.086(3)
V (Å^3)	12345(4)	11810.9(7)	11803(1)
ρ_{calcd} (g/cm^3)	4.893	5.951	5.280
μ (mm^{-1})	13.384	22.830	15.722
data/restraints/param	3285/0/133	3496 /0 /131	3505/0/133
GOF on F^2	1.008	1.067	1.079
final R indices R1/wR2 [$I > 2\sigma(I)$]	0.0355/0.0603	0.0294/0.0735	0.0327/0.0574
final R indices R1/wR2 (all data)	0.074/0.0635	0.0428/0.0993	0.0545/0.0646
largest diff peak, hole (e/Å^3)	3.507, −2.547	3.028, −4.165	3.762, −2.105

[a] Diffractometer refinement, hexagonal setting.

isotropic displacement parameters gave an improvement in R1 (0.055). However, the same ΔF peak had not changed and remained about 1.83 C from the fractional Zn13 position. Accordingly, this peak was refined as Zn15 at 42%, which reduced the largest peak to 6.32 e/Å^3 and 0.53 C from In3. A similar problem had been encountered for $K_{14}Na_{20}In_{96.30(1)}$,[8] in which split sites with 18% in each In were separated by 2.67 C. The separation in this Zn case is about 2.60 C. From the viewpoint of crystallography, both partially occupied Zn13 and Zn15 positions could also be refined as less occupied by In, which gives a different refined composition ($K_{34}In_{93.0}Zn_{8.1}$). However, subsequent powder diffraction for a product loaded with this composition showed only ~85% yield plus extra peaks from $K_{17}In_{41}$. Furthermore, this refined composition would correspond to six more valence electrons per cell than that in **III**, in which all bonding within clusters is already optimized at E_F (below). Final refinements of **III**, with anisotropic displacement parameters, converged at R1 = 0.033 and GOF = 1.079 for 133 variables and 3505 independent observed reflections ($I \geq 2\sigma_I$). The largest residual peak and hole in the ΔF map were 3.73 and −2.11 e/Å^{-3} at interatomic distances of 1.60 and 0.51 C from Zn12 and In5, respectively. Attempts to find a possibly better solution in lower-symmetry space groups *R*3*m*, *R*32, $R\bar{3}$, *R*3, *C*2/*m*, and even $P\bar{1}$ failed, and all still gave short distances for the fractional Zn15−Zn13 separation in the reported structure. The presence of a superstructure, which might generate the short distance and partial occupancy, was not supported by any additional Bragg reflections on the Stoe IPDS II diffractometer.

Second crystals of all three compounds were picked from other reactions in order to confirm the atomic positions and occupancies. These data were collected with the same conditions as before, but the final refinements of those data gave virtually identical results as before. Attempts to confirm compositions for all three compounds from energy dispersive spectroscopy (EDS) analyses failed because all of these compounds are very sensitive to traces of moisture and air. However, the major presence of Mg, Au, and Zn in **I**−**III**, respectively, was verified by the EDS analyses of the single crystals that were used for data collections.

Table 1 lists some crystallographic data for the three compounds, Table 2 gives the corresponding atomic positional, occupancy, and isotropic-equivalent displacement parameters, and Table 3 contains the important interatom distances for all three structures. The mixed or substituted sites are labeled with M or T (M = In/T and T = Mg, Au, Zn), respectively, and all are labeled in the same sequence as was used before.[8] More detailed crystallographic and refinement data and the anisotropic displacement parameters are available in the Supporting Information (CIF).

Physical Property Measurements. Electrical resistivities were measured by the electrodeless "Q" method with the aid of a Hewlett-Packard 4342A Q meter.[20] The method is particularly suitable for measurements on highly air-sensitive samples. For this purpose, 54.5 and 111.0 mg of powdered **I** and **II**, respectively, with grain diameters between 150 and 250 μm were dispersed with chromatographic alumina and sealed in Pyrex tubes. Measurements were made at 34 MHz over the range of 100−260 K. Measured resistivities for both increased linearly over the range, the change of which is taken as the defining characteristic of a metal, and the extrapolated ρ_{298} values were about 61.7 and 76.6 $\mu\Omega$ cm for **I** and **II**, respectively. Magnetic susceptibility data for **I** and **II** were obtained from 77.0 and 84.2 mg of ground powder, respectively, sealed under He in the container type described elsewhere.[21] The magnetizations were measured over the range of 6−330 K on a Quantum Design MPMS SQUID magnetometer. The magnetic susceptibility results for both compounds show almost temperature-independent paramagnetism over 50−330 K of about 1.3×10^{-3} and 2.5×10^{-3} emu/mol for **I** and **II**, respectively, after corrections were applied for the container, ion cores, and Larmor precession of the valence electron pairs in the large orbitals of each cluster.[22] Graphical data for these electrical resistivities and magnetic susceptibilities appear in the Supporting Information.

Band Structure Calculations. To assess chemical bonding characteristics of all three compounds, tight binding calculations were performed using the extended Hückel method with the *CAESAR* program package developed by Whangbo and coworkers.[23] According to Zintl−Klemm concepts, it is assumed that K atoms donate their electrons to the anionic lattice of the more electronegative elements, so these nuclei were not (and cannot be well) included in the EHTB calculations. The calculations for all three compounds were performed for their anionic networks with $P\bar{1}$ symmetry and with compositions close to the refined ones by treating some of the mixed positions as T (T = Mg, Au, or Zn) atoms and others as In. For example, for $K_{34}In_{91.05(9)}Mg_{13.95(9)}$, 42 of the total 315 atom positions in one unit cell ($Z = 3$) were treated as Mg and the others as In, with Mg positions being chosen to be nonadjacent. Only six k points were used for each because the unit cells are quite large. The following orbital energies and exponents were employed (Hii = orbital energy, eV; ξ = Slater exponent): In 5s, −12.6, 1.903; In 5p, −6.19, 1.677; Mg 3s, −9.00, 1.10; Mg 3p, −4.50, 1.10; Au 6s, −7.940, 2.12; Au 6p, −3.47, 1.5; Zn 4s, −12.41, 2.01; Zn 4p, −6.53, 1.7.[24,25] The d orbitals of Zn and Au

(20) Zhao, J. T.; Corbett, J. D. *Inorg. Chem.* **1995**, *34*, 378.
(21) Sevov, S. C.; Corbett, J. D. *Inorg. Chem.* **1991**, *30*, 4875.
(22) Selwood, P. W. *Magnetochemistry*, 2nd ed.; Interscience Publishers: New York, 1956; p 70. Ashcroft, N. W.; Mermin, D. N. *Solid State Physics*; Holt, Rinehart and Winston: Philadelphia, PA, 1976; p 649.
(23) Ren, J.; Liang, W.; Whangbo, M.-H. *CAESAR for Windows*; Prime-Color Software, Inc., North Carolina State University: Raleigh, NC, 1998.

Table 2. Atomic Positional Coordinates, Isotropic-Equivalent Displacement Parameters, and Site Occupancies for $K_{34}In_{91.05(9)}Mg_{13.95(9)}$ (**I**), $K_{34}In_{96.19(6)}Au_{8.81(6)}$ (**II**), and $K_{34}In_{89.95(1)}Zn_{13.05(7)}$ (**III**)

atom	*x*	*y*	*z*	*U*(eq)	Occ ≠ 1[a]
		Compound **I**			
In1	0.0102(1)	0.3680(1)	0.0365(1)	24(1)	
In2	0.1743(1)	0.0001(1)	0.3219(1)	22(1)	
In3	0.0397(1)	0.2519(1)	0.0782(1)	16(1)	
M4	0.2493(1)	0.0321(1)	0.1533(1)	20(1)	0.580/0.420(5)
In5	0.3874(1)	−*x*	0.1092(1)	15(1)	
In6	0.4457(1)	−*x*	0.0499(1)	13(1)	
In7	0.5402(1)	−*x*	0.0652(1)	27(1)	
In8	0.4204(1)	−*x*	0.1804(1)	12(1)	
In9	0.5696(1)	−*x*	0.1349(1)	14(1)	
In10	0.5117(1)	−*x*	0.1949(1)	12(1)	
In11	0.7544(1)	−*x*	0.2351(1)	15(1)	
M12	0.7208(1)	−*x*	0.1602(1)	19(1)	0.490/0.510(7)
M13	0.6102(1)	−*x*	0.2844(1)	29(2)	0.095/0.905(8)
In14	0	0	0.1131(1)	16(1)	
M15	0	0	0	24(2)	0.58/0.42(2)
K1	0.7957(1)	−*x*	0.0922(1)	34(2)	
K2	0	0	0.2609(1)	32(2)	
K3	0.5326(1)	−*x*	0.3449(1)	31(1)	
K4	0.0403(1)	0.4177(1)	0.1219(1)	14(1)	
K5	0.4458(1)	−*x*	0.2685(1)	16(1)	
K6	0	0	0.3618(1)	17(1)	
		Compound **II**			
In1	0.0114(1)	0.3693(1)	0.0366(1)	17(1)	
In2	0.1739(1)	0.0007(1)	0.3219(1)	20(1)	
In3	0.0328(1)	0.2495(1)	0.0791(1)	19(1)	
In4	0.2437(1)	0.0346(1)	0.1520(1)	20(1)	
In5	0.3875(1)	−*x*	0.1090(1)	12(1)	
In6	0.4447(1)	−*x*	0.0506(1)	14(1)	
In7	0.5397(1)	−*x*	0.0657(1)	18(1)	
In8	0.4200(1)	−*x*	0.1804(1)	12(1)	
In9	0.5710(1)	−*x*	0.1352(1)	20(1)	
In10	0.5106(1)	−*x*	0.1956(1)	16(1)	
M11	0.7530(1)\	−*x*	0.2352(1)	22(1)	0.243/0.757(7)
M12	0.7211(1)	−*x*	0.1580(1)	20(1)	0.455/0.545(7)
In13	0.6096(1)	−*x*	0.2810(1)	25(2)	
In14	0	0	0.1165(1)	50(1)	
Au15	0	0	0	18(2)	
K1	0.7966(1)	−*x*	0.0935(1)	34(2)	
K2	0	0	0.2582(1)	37(2)	
K3	0.5353(1)	−*x*	0.3465(1)	34(1)	
K4	0.0387(1)	0.4167(1)	0.1226(1)	19(1)	
K5	0.4458(1)	−*x*	0.2686(1)	19(1)	
K6	0	0	0.3623(1)	22(1)	
		Compound **III**			
In1	0.0105(1)	0.3672(1)	0.0370(1)	19(1)	
In2	0.1739(1)	−0.0002(1)	0.3223(1)	20(1)	
In3	0.0375(1)	0.2445(1)	0.0773(1)	25(1)	
In4	0.2432(1)	0.0345(1)	0.1527(1)	19(1)	
In5	0.3872(1)	−*x*	0.1099(1)	21(1)	
In6	0.4454(1)	−*x*	0.0513(1)	20(1)	
In7	0.5412(1)	−*x*	0.0662(1)	22(1)	
In8	0.4201(1)	−*x*	0.1802(1)	18(1)	
In9	0.5744(1)	−*x*	0.1358(1)	18(1)	
In10	0.5114(1)	−*x*	0.1949(1)	16(1)	
M11	0.7500(1)	−*x*	0.2367(1)	30(1)	0.658/0.342(9)
Zn12	0.7168(1)	−*x*	0.1624(1)	32(1)	
Zn13	0.6120(1)	−*x*	0.2873(1)	43(1)	0.695(5)
In14	0	0	0.1141(1)	42(1)	
Zn15	0	0	0.0324(3)	104(6)	0.42(1)
K1	0.7958(1)	−*x*	0.0941(1)	34(1)	
K2	0	0	0.2593(1)	35(1)	
K3	0.5324(1)	−*x*	0.3444(1)	37(1)	
K4	0.0368(1)	0.4148(1)	0.1226(1)	17(1)	
K5	0.4458(1)	−*x*	0.2678(1)	17(1)	
K6	0	0	0.3632(1)	20(1)	

[a] Only co-occupancies for M = In/T (T = Mg, Au, or Zn) or partial occupancies for Zn are shown. Sites are uniformly numbered for all three phases.

Table 3. Selected Bond Distances (Å) in $K_{34}In_{91.05(9)}Mg_{13.95(9)}$ (**I**), $K_{34}In_{96.19(6)}Au_{8.81(6)}$ (**II**), and $K_{34}In_{89.95(1)}Zn_{13.05(7)}$ (**III**)

bond	I	II	III
In1−In1	2.977(1)	2.944(1)	2.988(1)
In1−In3	3.018(1)	2.970(1)	3.0167(9)
In1−In6	3.075(1)	3.0308(9)	3.0487(8)
In1−In2	3.075(1)	3.059(1)	3.0549(9)
In1−In7	3.183(1)	3.1337(9)	3.1706(8)
In1−In2	3.239(1)	3.187(1)	3.2013(9)
In2−In7	3.011(1)	2.996(1)	2.992(1)
In2−In6	3.084(1)	3.061(1)	3.075(1)
In2−In2	3.267(2)	3.187(1)	3.203(1)
In3−M11	2.913(1)	2.8054(8)	2.7878(8)
In3−M13	3.022(4)	2.951(1)	2.944(2)
In3−In10	3.075(1)	3.064(1)	3.090(1)
In3−In3	3.237(1)	3.396(1)	3.124(1)
In3−M4	3.258(1)	3.111(1)	3.234(1)
M4−M4	2.936(3)	3.099(1)	3.088(1)
M4−M12	2.984(2)	2.8487(9)	2.885(1)
M4−M11	3.071(1)	2.9205(9)	3.021(1)
M4−In10	3.096(1)	3.1065(9)	3.0869(8)
M4−In9	3.233(1)	3.176(1)	3.1505(8)
M4−M4	3.471(3)	3.222(1)	3.213(1)
In5−In5	3.039(2)	3.000(1)	2.981(1)
In5−In8	3.044(1)	2.9900(9)	2.9828(9)
In5−In6	3.062(1)	2.966(1)	2.991(1)
In5−In8	3.080(1)	3.042(1)	3.010(1)
In6−In7	3.131(2)	3.100(1)	3.117(1)
In7−In9	2.981(1)	2.950(1)	2.986(1)
In8−In8	3.038(1)	2.986(1)	2.974(1)
In8−In10	3.024(1)	2.962(1)	2.975(1)
In9−M12	2.922(1)	2.8113(9)	2.768(1)
In9−In10	3.074(1)	3.092(1)	3.110(1)
M11−In14	2.913(1)	2.8593(9)	2.753(1)
M11−M13	3.203(4)	3.0447(9)	3.100(2)
M11−M12	3.228(2)	3.250(1)	3.163(2)
M12−M12	3.045(3)	3.016(1)	2.772(3)
M12−In14	3.003(3)	2.925(1)	2.786(2)
M13−M13	3.176(8)	3.165(1)	3.026(4)
M13−In14	3.185(5)	3.148(2)	3.240(3)
M13−M15	2.701(5)	2.777(1)	1.830(4)
Zn15−Zn15			2.60(2)

were not included in the calculations after it was discovered that these were well removed from the Fermi level. Both the relativistic and nonrelativistic energies and orbital exponents for Au[25] were tried, but they gave virtually the same results.

Results and Discussion

Crystal Structures. $K_{34}In_{91.05(9)}Mg_{13.95(9)}$ (**I**) and $K_{34}In_{96.19(6)}Au_{8.81(6)}$ (**II**) are isostructural with $Na_{102}(MGa)_{315}$ (M = Cu, Zn)[7] and $A_{34}(In, Li)_{105}$ (A = K and/or Na)[8] but with different mixed sites. $K_{34}In_{89.95(1)}Zn_{13.05(7)}$ (**III**) is very similar to $K_{14}Na_{20}In_{96.30}$ except for some split sites only in the latter.[8] All three compounds have basically the same general structure (Figure 1), in which three-dimensional anionic networks are composed of two types of interbonded empty In_{12} icosahedra A (green) and B(red) and complex C (blue) building blocks. The symmetry and atom labels in each polyhedron are given in the Supporting Information (Figure S1). Complex C in **III** is different from those in the other two compounds, but all of them are formed from pairs of triply fused icosahedron. This M_{28} unit originates from a single icosahedron by action of a central 3-fold axis through the shared atom In14 to generate shared faces of M11−

(24) Canadell, E.; Eisenstein, O.; Rubio, J. *Organometallics* **1984**, *3*, 759.
(25) Assfa, Z.; DeStefano, F.; et al. *Inorg. Chem.* **1991**, *30*, 2868.

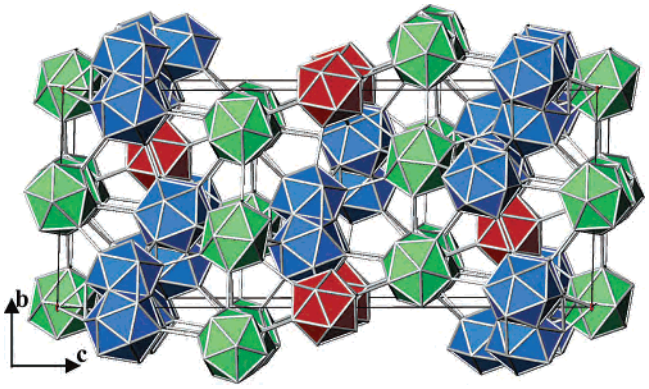

Figure 1. ~[100] view of the unit cell of $K_{34}In_{91.07}Mg_{13.93}$(**I**) with three different cluster types: icosahedra A (green) and B (red) and sandwich complex $(M_{28})M(M_{28})$ (blue). K atoms are omitted for clarity.

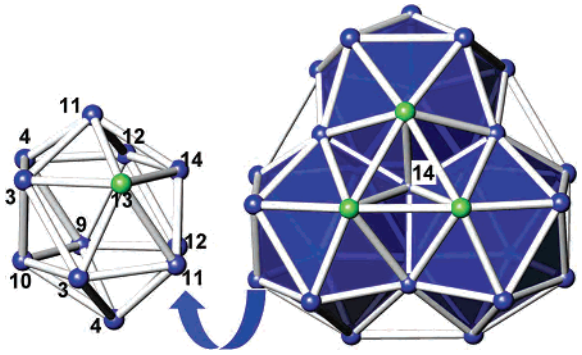

Figure 2. Triply fused icosahedron M_{28} generated from a single icosahedron by means of a 3-fold axis through the shared In14 atom.

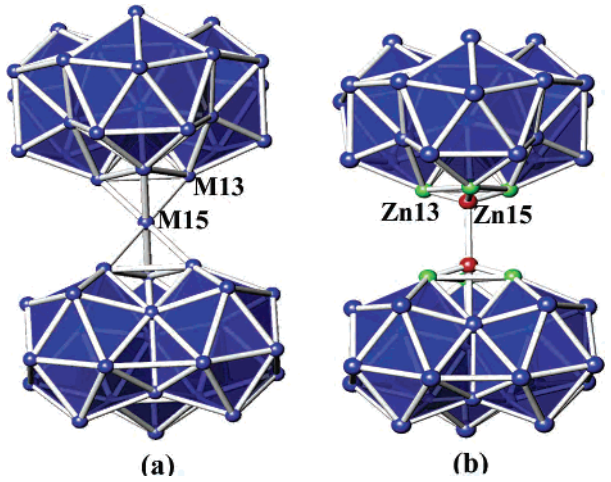

Figure 3. (a) Sandwich complex $(M_{28})M(M_{28})$ around a six-coordinate M15 atom in **I** and **II**. (b) Two M_{28} fused polyhedra interconnected by a Zn−Zn dimer in **III**, in which both Zn13 (green) and Zn15 (red) sites are partially occupied.

M12−In14 (Figure 2). Neighboring pairs of triply fused icosahedra in **I** and **II** are interconnected by an atom M15 (at the 3*a* Wykoff site 0,0,0) to form a sandwich complex $(M_{28})M(M_{28})$ (Figure 3a). In **III**, the Zn15 position locates at a 6*c* site off of the inversion center to produce two triply fused icosahedron interconnected by a Zn15−Zn15 dimer (2.60 C; Figure 3b). The separation of the M_{28} polyhedra in the presence of small Zn in **III** is further increased by relaxation of the complex through enlargement of the triangle that is capped by a fractional interconnected atom (Zn15). Compared with Mg in **I**, a single interconnecting Zn atom in **III** would be too small to separate the two M_{28} units (metallic radii, Zn = 1.213 C and Mg = 1.364 C).[26]

The cations in all three compounds effectively center different polyhedra. For both **I** and **II**, K4, K5, and K6 each center one M_{12} Friauf polyhedron, K1 atoms center a larger M_{16} polyhedron, and K2 and K3 each center M_{15} polyhedra (all are illustrated in Figure S2 of the Supporting Information). For **III**, all polyhedra around each K are the same as those in **I** and **II** except for the one centered by K3, which becomes an M_{17} polyhedron because of the pairs of M15 atoms. In all three phases, the larger volumes around the K1−K3 atoms allow these larger thermal parameters and greater distances to In compared with those around K4−K6, as shown in Tables 2 and 3. For example, in compound **II**, the average distance to In about K1−K3 is 3.87 C, and for K4−K6, 3.59 C. Larger displacement parameters and greater distances around the K1−K3 positions have been observed in all tri-icosahedral phases.[7−9] The shorter K−In distances around K4−K6 make it possible for these positions to be occupied by smaller Na, as was found earlier for $K_{14}Na_{20}In_{91.82}Li_{13.18}$ and $K_{14}Na_{20}In_{96.30}$.[8] However, attempts to substitute those K positions by Na in the current compounds failed.

The networks formed by cations in all three compounds have the same characteristics. All K atoms surmount triangular faces of icosahedra and triply fused icosahedra to form pentagonal dodecahedra K_{20} and hexakaidecahedra K_{28}, respectively. As discussed before, these polyhedra further define a K_{136} clathrate-II type network in $K_{17}In_{41}$, $K_{39}In_{80}$, $K_{22}In_{39}$ $Na_{22}Ga_{39}$, $Na_{35}Cd_{24}Ga_{56}$, $K_{21-\delta}Na_{2+\delta}In_{39}$ ($\delta = 2.8$), and $Na_{12}K_{18}In_{53}Tl_7$.[8,27] The presence of these regular cation arrangements is probably decisive in the formation of the basic structures.

Triply Fused Icosahedra. These were first found in β-B and in isotypic triel clusters in alkali−metal−triel (Ga, In) systems. All examples of triply fused icosahedra have either partial occupancies of some atom positions or mixtures of triel with electron-poorer atoms therein that reduce electron counts and serve to stabilize the large clusters. The main differences among all tri-icosahedron phases are the interconnections between pairs of neighboring triply fused icosahedra, which are dependent on the intervening M15 (Figure 3). Three kinds of interconnection have been found: a single six-coordinate atom M15 (3*a*); an M15−M15 dimer (6*c*); or no M15 interconnection at all. The refined position of M15 is related to the occupancy of M13 atoms. When the M13 site is fully occupied, a single M15 position occurs at the 3*a* site at the origin, always with full occupancy, such as in **I**, **II**, and several other tri-icosahedral phases: $Na_{102}(MGa)_{315}$ (M = Cu, Zn),[7] $K_{34}In_{92.30}Li_{12.70}$, and $K_{14}Na_{20}In_{91.82}Li_{13.18}$.[8] In the case of partial M13 occupancy, M15 is found

(26) Pauling, L. *Nature of the Chemical Bond*, 3rd ed.; Cornell University Press: Ithaca, NY, 1960; p 403.
(27) Li, B.; Corbett, J. D. *Inorg. Chem.* **2003**, *42*, 8768. Carrillo-Cabrera, W.; Caroca-Canales, N.; von Schnering, H.-G. *Z. Anorg. Allg. Chem.* **1994**, *620*, 247.

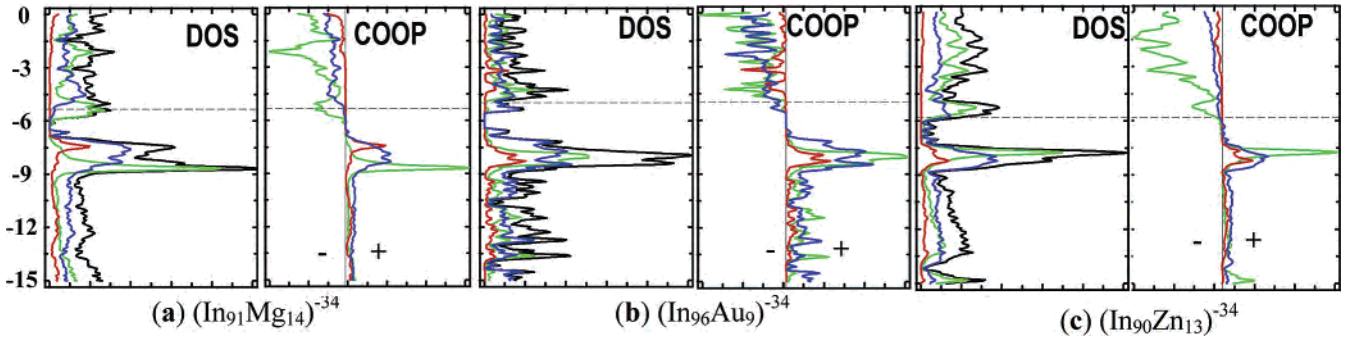

Figure 4. DOSs for anion frameworks and COOP data for bonds within cluster units for compounds **I** (a), **II** (b), and **III** (c). Data for icosahedra A and B and large fused complex C are green, red, and blue, respectively, and the total DOS is black. The dotted lines denote the Fermi energies.

at the 6*c* site to give a dimer interconnection. In **III**, the M13 position is only 70% occupied by Zn, and each Zn15 atom would be impossibly close to M13, 1.83C at full occupancy, which explains the considerably larger displacement parameters of Zn15. With less occupancy of In (50%) at the M13 position, $K_{14}Na_{20}In_{96.30}$ also shows a dimer interconnection.[8] When the occupancy of Ga13 becomes only 19% in $K_4Na_{13}Ga_{49.57}$, no Ga15 position is found, and there is no interconnection between neighboring triply fused icosahedra.[9]

Mixing of In and T Elements. All three reported compounds, as with $A_{34}(In,Li)_{105}$ (A = K, Na), have some In positions in the new tri-icosahedral phases substituted with different group elements (T), i.e., Li, Mg, Au, or Zn. Mulliken electronegativities[28] for the neutral atoms involved are as follows: Li, 3.01; Mg, 3.75; Au, 5.77; Zn, 3.2. That of Li is larger than that of K (2.42) and close to that of In (3.1); therefore, the preferred electron donor in these K−T−In systems is K, and T instead mixes with In at the cluster sites. However, all four T elements show more or less different substitution patterns; Li compounds substitute within both complex C and icosahedron A, but in all three compounds reported here, T mixes only in complex C. Similar mixing sites are still shown between compounds with neighboring group relationships: Li−Mg and Zn−In. Both Mg and Li compounds show mixing at the three sites: M4, M12, and M13. In contrast, both $K_{34}In_{89.95(1)}Zn_{13.05(7)}$ and $K_{14}Na_{20}In_{96.30}$ exhibit partial occupancies at the M13 and M15 sites, and similar structures are mainly characterized by the dimer-interconnected triply fused icosahedra. On the other hand, Au shows quite different site occupancies: only the M11 and M12 sites contain mixed In/Au, and the M15 site is fully occupied by Au. The different atom sizes, electronegativities of these elements, and site preference energies[29] are thought to be responsible for these diverse patterns.

Electronic Structure and Chemical Bonding. Extended Hückel band calculations have been performed for all three compounds in order to understand differences in the chemical bonding in these three compounds, particularly, as to why these compounds have more valence electrons (1005−986 per cell) than the isostructural $K_{34}In_{92.30}Li_{12.70}$, $K_{14}Na_{20}In_{91.82}Li_{13.18}$, and $K_{14}Na_{20}In_{96.30}$, which all have ∼970 electrons.[8] Parts a−c of Figure 4 illustrate the densities-of-state (DOSs) and crystal orbital overlap population (COOP) results for the anion portions of **I**−**III**, respectively. The DOS curves describe the total DOS and the partial projections for icosahedra A (red) and B (green) and complex C (blue), and the COOP data show the corresponding bonding interactions within the same three units.

According to the DOS curves, both **I** and **II** have an energy gap, or nearly so, at an energy corresponding to about 960 valence electrons per cell. This optimum is consistent with empirical electron counting by means of the *mno* rule.[8,10] The sandwich complex $(M_{28})M(M_{28})$ unit requires $m + n + o = 8 + 57 + 1 = 66$ skeletal electron pairs, i.e., 132 electrons, for stability. In both the Mg and Au compounds, all positions are fully occupied, and with nine 12-bonded In_{12} A, three 12-bonded In_{12} B, and three 36-bonded $(M_{28})M(M_{28})$ units per cell ($Z = 3$), the number of valence electrons to fill all of the bonding levels is $9(26 + 12) + 3(26 + 12) + 3(132 + 36) = 960$. The partial occupancies in **III** make empirical electron counting harder, but the DOS curve (Figure 4c) shows a pseudo-gap corresponding to ∼958 valence electrons per cell. However, the experimental valence electron counts per cell (1005.2, 994.1, and 986.4 for Mg, Au, and Zn phases, respectively) are greater, and so their Fermi levels intersect finite DOS. This empirical metallic character so predicted for **I** and **II** is in agreement with the measured properties (Supporting Information). For both **I** and **III**, the DOS cut mainly through the states of the In_{12} icosahedron A and of complex C in **II**. The COOPs for all three indicate that all metal−metal bonding within complex C is effectively optimized crossover at E_F. The small antibonding effect within complex C in the Au compound might be related to the relativistic effect of Au. On the other hand, semiempirical methods such as extended Hückel may not accurately assess the bonding character. These compounds are likely metallic, but, contrariwise, the calculations treat all states as relatively localized; furthermore, site preference energies[29] were not considered but rather only bonding energies. Theoretical calculation with the use of relativistic density functional theory methods would probably provide some important calibration for the simpler extended Hückel calculations.[30]

(28) Pearson, R. G. *Inorg. Chem.* **1988**, *27*, 734.
(29) Miller, G. J.; Choe, C.-S. *Highlights in Inorganic Chemistry*; Meyer, G., Naumann, D., Wesemann, L., Eds.; Wiley-VCH: New York, 2001; Chapter 2.

Conclusions. In this paper, we present the syntheses and structures of three new alkali−metal−In compounds, all of which exhibit complex three-dimensional anionic networks built of In_{12} icosahedra and $(In, T)_{28}$ triply fused icosahedra (T = Mg, Au, or Zn). This is another good example in which electronic tuning among the complicated network structure is realized by substitution of part of In atoms by electron-poorer T atoms along with structural perturbations caused by electronic requirements. These parallel the discovery and analysis of the $K_{34}In_{92.30}Li_{12.70}$ system.[8] Only a line phase is observed in each compound with a certain amount of T element substitution, which holds true for all tri-icosahedral phases. It is also interesting to notice that some In positions in this complex structure can be substituted with different group elements, such as Li, Mg, Au, and Zn, but with different mixing patterns, and the substitutions apparently provide just enough reduction in the valence electron counts to optimize the metal−metal bonding within the complexes.

Acknowledgment. We are indebted to S. Budko for the magnetic susceptibility data.

Supporting Information Available: X-ray crystallographic files in CIF format for the three structures, two explanatory pictures of the structures, and plots of resistivity and magnetic susceptibility data for **I** and **II**. This material is available free of charge via the Internet at http://pubs.acs.org.

IC061089Y

(30) Ziegler, T.; Nagle, J. K.; Snijders, J. G.; Baerends, E. J. *J. Am. Chem. Soc.* **1989**, *111*, 5631. Mudring, A.-V.; Corbett, J. D. *J. Am. Chem. Soc.* **2004**, *126*, 5277.